Computer-aided detection of wall motion abnormalities in cardiac MRI

Suinesiaputra, A.

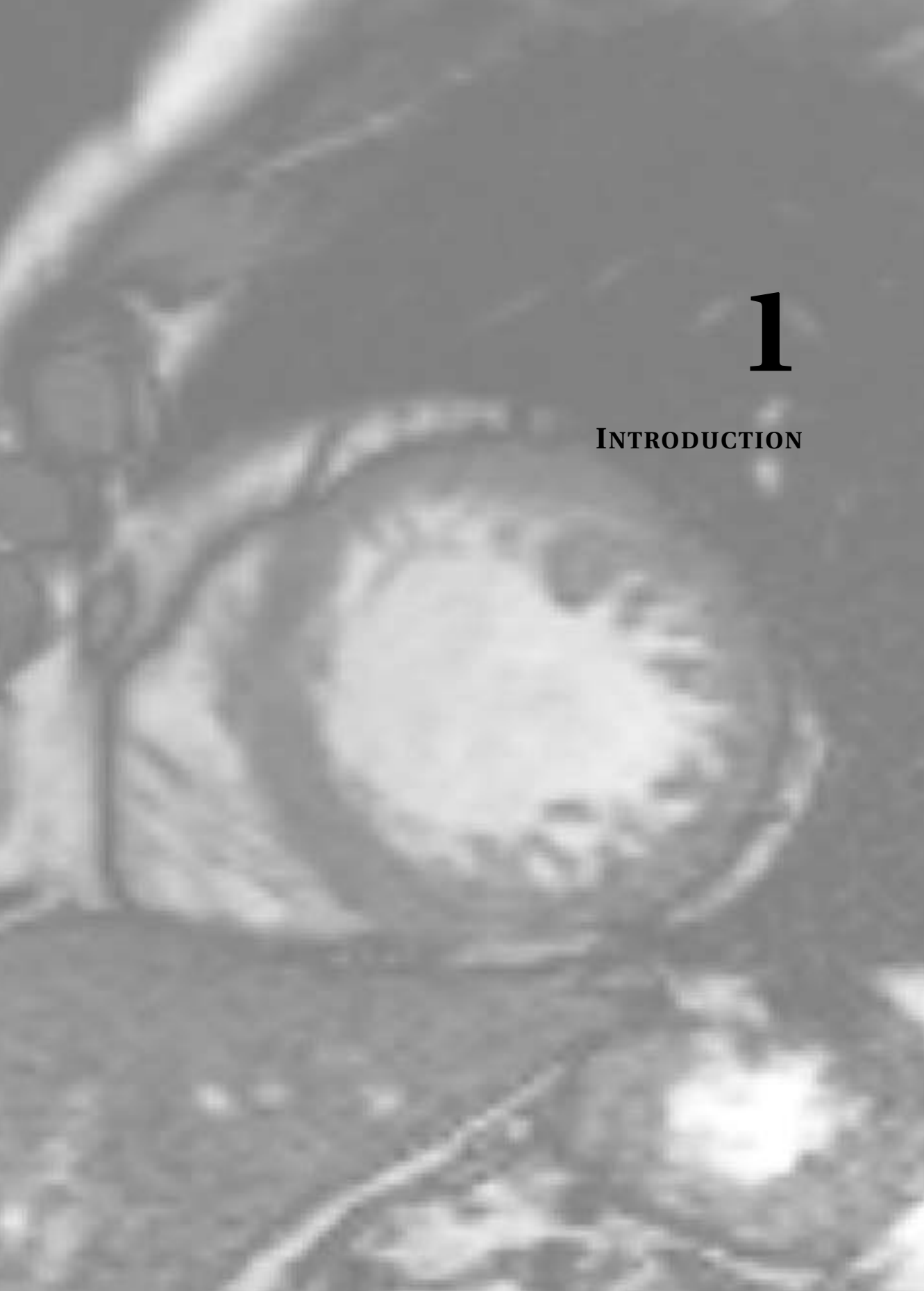

1

Introduction

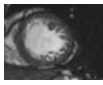

Melman: Yeah. I often doze off while I'm getting an MRI.
Alex: Melman, you're not getting an MRI!
Melman: CAT scan?
Alex: No! No CAT scan! It's a zoo transfer!
Melman: ZOO TRANSFER?!

MADAGASCAR (2005)

CORONARY artery disease is a condition in which plaque builds up inside the coronary arteries, causing disruption of the supply of oxygen-rich blood to the myocardium. The prevalence, incidence, hospitalization rate and costs of this disease in the developed countries have steadily increased [1]. It has been a leading cause of death in Europe and North America, and it may even accelerate the progression of heart failure, and as such, it is responsible for 70% of congestive heart failure cases [2].

Ischaemia is a condition of the heart when the supply of blood to the myocardium is significantly reduced, mainly as the result of coronary artery disease. The imbalance in supply and demand of oxygen in the circulation leads to functional sequelae known as the ischaemic cascade. This starts with perfusion abnormalities, metabolic changes (*silent ischaemia*), wall motion abnormalities, diastolic dysfunction, systolic dysfunction, angina and ultimately infarction [3, 4]. As a result of chronic contractile dysfunction, myocardium may turn into a hibernating state. Hibernating myocardium is an equilibrial condition after prolonged subacute or chronic ischaemia in which metabolism and contractile function are reduced to match the blood supply. The hibernating myocardium is capable of returning to normal or near-normal function after restoration of an adequate blood supply [5]. Hibernating myocardium thus suggests the presence of viable tissue, which may gain functional improvement after treatment [6]. In the absence of a significant amount of viable myocardium, restoring the blood flow is not beneficial anymore. Assessment of dysfunctional but viable myocardium has become an important determinant in the prognosis of ischaemic heart disease for long term survival.

A common treatment for restoring blood flow to the heart is coronary revascularization. Two common revascularization procedures are coronary artery bypass grafting (CABG) and percutaneous coronary intervention (PCI). CABG restores blood flow of an obstructive coronary artery by rerouting the artery with a new vessel. PCI is performed by angioplasty, i.e., threading a balloon-tipped tube to be inflated, compressing the plaque and dilating the narrowed coronary artery to improve the blood flow again, and then followed by vascular stenting to keep the vessel open. Although overall survival has improved due to these revascularization treatments, the result remains a partial success [7]. This emphasizes the need for and the importance of an early and noninvasive diagnosis and quantification of ischaemic heart disease.

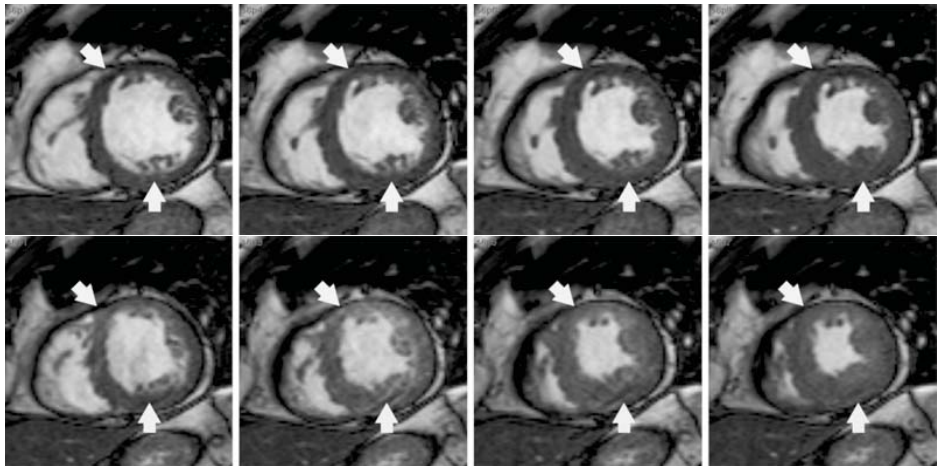

FIGURE 1.1: Resting (TOP) and dobutamine stress (BOTTOM) cine-MR images from the same patient at a single MR acquisition session. An increase of dobutamine-induced wall thickening is visible at the inferior region (the bottom arrows). This indicates a possible viable myocardium. At the anteroseptal region (the top arrows), there is no increase of LV function from rest to stress, which suggests non-viable tissue.

1.1 Imaging techniques for diagnosis of ischaemic heart disease

In the last few decades, an enormous amount of research has been carried out towards imaging of ischaemic heart disease. Different image acquisition approaches have emerged, either to detect the disease before symptoms occur, to assess the presence and the extent of the disease in the symptomatic patient, or to monitor the disease progression over time. Particularly for viability assessment, hibernating myocardium can be traced with some imaging techniques, which can detect either the presence of myocardial tissue that contracts if stimulated (wall motion analysis) or the persistence of metabolic activities within the regions of dysfunctional myocardium (perfusion analysis).

Though head-to-head comparisons between imaging techniques have been performed with respect to viability, no single test has been reported to have a perfect or nearly perfect sensitivity and specificity [8]. An integrated use of different image acquisitions is therefore needed in clinical decision making [8, 9]. In the following sections, clinical applicability of different image modalities to assess ischaemic heart disease is briefly presented.

1.1.1 Magnetic resonance imaging (MRI)

MRI has a unique position in the management of ischaemic heart disease because it is the only single image modality that allows visualization of all ischaemic events through

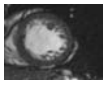

different MR protocols [3]. In a single session, perfusion defects, resting cardiac function, stress imaging and infarct images can be acquired with MRI [2, 4, 10]. Hence, MRI has the potential to be implemented as a "one-stop shop" imaging modality for the diagnosis of ischaemic heart disease.

1.1.1.1 Resting cine-MR images

Cine MR images are generally used in standard clinical practice for quantification of global and regional LV functions, e.g., ejection fraction, stroke volume, wall thickening, and wall thickness, because of its superb contrast delineation of myocardium with the blood pool, right ventricle and other tissues. Cine MR imaging captures a full cardiac cycle in an MR time sequence. Hence, cine MRI allows quantification of wall motion as well as end-diastolic wall thickness (EDWT) and systolic wall thickening (SWT), which are key functional parameters for quantifying ischemic heart disease.

1.1.1.2 Dobutamine stress MR (DSMR)

In the assessment of myocardial viability, the presence of contractile reserve is frequently used to identify viable myocardium. Contractile reserve can be assessed by low dose dobutamine injection prior to MR acquisition, which will produce cardiac stress MRI [2, 11]. Contractile reserve is shown by the increase of the dobutamine-induced systolic function compared against the corresponding resting cine-MRI.

The diagnostic procedure with DSMR starts from visual wall motion scoring of myocardial segments in resting MR. Four visual score levels are defined: *normokinetic* (normal), *hypokinetic* (reduced), *dyskinetic* (abnormal) and *akinetic* (no contraction). The hypokinetic score may sometimes be divided into *mild* and *severe* hypokinetic. Subsequently, observers predict functional improvement in non normokinetic segments by comparing cine MR sequences between resting MR and DSMR. Figure 1.1 shows an example of a comparison between resting and dobutamine-stress cine MRI. Observer experience inevitably affects the diagnostic quality of DSMR [12, 13]. Quantitatively, viable myocardium can also be characterized by the preserved EDWT and SWT from rest to stress MR [14, 15].

1.1.1.3 MR perfusion

An MR perfusion study is performed by the injection of gadolinium pentaacetic acid (Gd-DPTA) prior acquisition. The contrast agent enables full inspection of myocardial tissue perfusion during the first-pass myocardial intensity enhancement (see Figure 1.2). First-pass MR perfusion images are usually evaluated by an upslope analysis of myocardial time-intensity curves.

Coronary artery disease can be assessed by the combination of rest and stress perfusion studies [16, 17]. During stress, the blood flow through myocardium increases three- to fourfold. The ratio of the maximum blood flow to the baseline, known as myocardial perfusion reserve index (MPRI), has been used as an index of functional severity of a coronary lesion [18].

1.1.1.4 Contrast-enhanced MRI (CE-MRI)

Following a rest MR perfusion study, the amount of washed-out contrast agent inside myocardium can be quantified. In an infarcted region, extracellular contrast agent passively diffuses into the intercellular space due to myocyte death. This accumulation of contrast agent increases tissue-level contrast. Chronic infarcts are characterized by the absence of living myocytes, which widens interstitial space between collagen fibres. This increases contrast agent concentration that results in hyperenhancement [2]. Figure 1.3 shows an example of a contrast-enhanced MRI in which hyperenhancement is notably present at the anterior region of the myocardium.

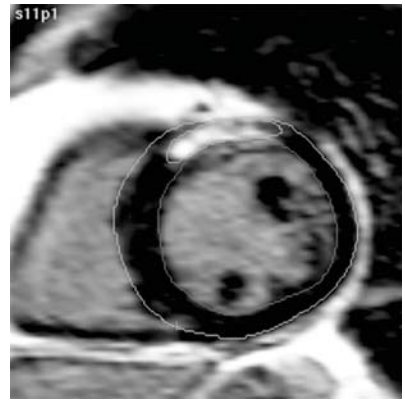

FIGURE 1.3: An example of CE-MRI.

Typically, a contrast-enhanced MR acquisition is performed 10–20 minutes after the intravenous introduction of the contrast agent and therefore CE-MRI is often referred to delayed-enhancement or late-enhancement MRI. CE-MRI is effective in identifying the presence, location and extent of acute and chronic myocardial infarction. Transmural extent has become the main metric of infarct assessment in CE-MRI, because there is a strong correlation between infarct transmurality and the infarct size [19].

Additionaly, CE-MRI allows prediction of functional improvement in ischaemia. Viable and non-viable tissue can be distinguished by setting a threshold value on infarct transmurality. However, it is still an open debate how to define this threshold value; some define a transmural extent of less than 75% as viable [11, 20, 21], while others prefer a more moderate 50% threshold value [22–24].

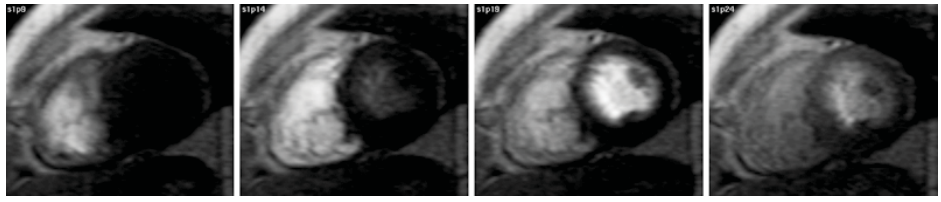

FIGURE 1.2: A sequence of first-pass MR perfusion images. The paramagnetic contrast agent starts entering the right ventricle (LEFTMOST), fills the right ventricle and then left ventricle before it leaves the ventricle completely (RIGHTMOST). Image courtesy of Vikas Gupta, LKEB, LUMC, the Netherlands.

1.1.2 Echocardiography

Echocardiography has gained much popularity for the assessment of ischaemic heart disease because it is a noninvasive low-cost imaging technique that is available in many clinical scenarios. Echocardiographic imaging can also assess tissue viability through different protocols [25, 26], i.e. dobutamine stress echocardiography, tissue doppler imaging and myocardial contrast echocardiography.

Dobutamine stress echocardiography (DSE) assesses the functional response of the heart at stress after the administration of low-dose dobutamine infusion. Viability is noted in DSE by the improvement of ejection fraction from rest to stress, which is directly related to the number of myocardial segments with contractile reserve [27]. Applying DSE in patients with poor acoustic window however is still problematic. DSE suffers from low interobserver and interinstitutional agreement due to different interpretations of stress echocardiograms [28, 29]. Better standardization of visual assessment [30], which can be assisted by an automated method [31], is needed to allow objective evaluation of viable tissue with DSE.

Tissue Doppler imaging (TDI) is a color Doppler imaging technique which analyzes point velocities, accelerations and Doppler signal strength in the myocardium instead of in the blood pool [32]. Several efforts have been made to exploit TDI for viability assessment, but inconsistent prediction of functional recovery from TDI parameters was found [25]. From TDI, strain and strain rate imaging can be derived. Strain rate of scar tissue deteriorates as the extent of infarct transmurality increases and this measurement can improve the accuracy of TDI to assess viability [33]. The main drawback of TDI is the continuum of velocity measurements that often produces false abnormal velocity of a normal segment tethered by jeopardized neighboring segments.

Myocardial contrast echocardiography (MCE) is another echocardiographic imaging protocol that measures cellular viability in myocardium. Myocardial necrosis is associated with the loss of microvasculature, which can determine viable and non-viable tissue [34].

1.1.3 ^{18}F-fluorodeoxyglucose (FDG) PET imaging

Under normal resting conditions, free fatty acid (FFA) and glucose are two main energy sources of cardiac metabolism. Under ischaemia, oxygen supply decreases which reduces metabolism of FFA. Consequently, exogenous glucose becomes the primary metabolic substrate for myocardium [35]. The increase of glucose uptake by myocardium is therefore an important indicator for ischaemia.

Glucose metabolism in the organ system can be traced by the glucose analog 2-[F-18]-2-deoxy-2-fluoro-D-glucose (FDG) uptake. Myocardial FDG uptake can be imaged by using positron emission tomography (PET). For predicting LV functional improvement after revascularization, FDG-PET has been regarded as the standard of reference for other imaging techniques [36] However, its limited availability and high costs hamper its application for daily clinical routine.

Cardiac FDG-PET images are relatively low resolution and lack anatomical detail. To provide morphological information, FDG-PET imaging is sometimes combined with other

imaging modalities, such as MR or CT images [37–41]. This approach requires a good registration method to allow an accurate quantitative analysis.

1.1.4 Electrocardiographically-gated perfusion SPECT imaging

Electrocardiographically-gated SPECT (radionuclide perfusion imaging) is a tomographic imaging technique with a radioisotope perfusion tracer. The acquisition is controlled by electrocardiography (ECG) to generate full cardiac cycle of perfusion images [42, 43]. Three perfusion tracers: ^{99m}Tc-sestamibi, ^{99m}Tc-tetrofosmin and ^{201}Ti (Thallium), are routinely used in clinical practice. Standard myocardial perfusion SPECT can be performed at rest or after pharmacologically induced stress. ECG-gated SPECT imaging provides several prognostic values for ischaemic heart disease, including myocardial viability [44, 45] and disease monitoring following a revascularization procedure [46–48].

1.2 Computer-assisted diagnosis for ischaemia

The first articles of computerized methods for analyzing medical image data appeared in the 1960s [49, 50], which marked the beginning of CAD development. Initially, a considerable optimism was exalted that a computerized method could provide a complete diagnosis. This expectation gradually abated over time. Instead of assigning the computer the role of a diagnostician, CAD methods have gradually shifted towards computer-generated diagnostic systems to support the physicians' own assessment [51]. A modern CAD method acts as a *second reader* that automatically highlights candidates of a lesion, providing a second opinion to the first reader (radiologist/clinician).

The role of CAD as a second reader has been fostered for the detection of lesion, that are prone to be missed by radiologists alone. That includes the detection of pulmonary nodules in chest radiographic images [52–56], the detection of colorectal polyps from CT colonographic images (virtual colonoscopy) [57–60], and the detection of breast cancer from mammography in breast screening programs [61–63]. A large body of research has been published in these fields, resulting in hundreds of proposed CAD methods with varying results [64, 65]. Common in these results was a substantial increase of sensitivity by the CAD-supported assessment, although the increase varied with the experience of the reader. The advent of CAD has helped radiologists to reduce their reading time [58, 66, 67] and it has also decreased interobserver variability among readers [68, 69].

Also in other areas, several attempts have been made to develop a CAD system to detect lesions or abnormalities. CAD was applied to identify suspected intracranial aneurysms in MR angiographic images [70, 71], to detect pulmonary embolisms [72], to identify arteriolar narrowing in fundus images [73], and mainly other tumor detection applications.

For cardiac applications, a simple computer-aided detection system cannot be applied because of the dynamic nature of the heart. A CAD system for heart disease must be based on what is known as *differential diagnosis* [65], which is based on quantitative differences between two reference points. Currently, CAD for ischaemic heart disease is still in its infancy. Most of the proposed automated methods focused on presenting direct

TABLE 1.1: Comparison of existing automated wall motion assessment methods.

	Method	Regional	Modality	Sample size
Douglass et. al. [90]	LDA	yes	gated SPECT	31
Remme et. al. [91]	SSM	no	cine MRI	13
Bosch et. al. [78]	SSM	yes (limited)	DSE	64
Herz et. al. [92]	PI	yes	3D echo	1 (canine)
Ruiz Dominguez et. al. [93]	PI	yes	echo	10
Caiani et. al. [94]	TV	yes	cine MRI	18
Kachenoura et. al. [95]	PI	yes	cine MRI	13
Lekadir et. al. [88]	SSM	yes	cine MRI	40
Qazi et. al. [96]	LDA	no	echo	—
Leung et. al. [97]	SSM	yes	DSE	129
Mansor et. al. [98]	HMM	yes	DSE	44
Suinesiaputra et. al. [99, 100]	SSM	yes	cine MRI	45

LDA = linear discriminant analysis, SSM = statistical shape model, PI = parametric image,
TV = threshold value, HMM = hidden markov model

raw quantification of global or regional LV function to the clinicians [74, 75]. Much effort has been spent on the development of automated quantification of cardiac images, which includes segmentation, registration and cardiac modeling [76, 77].

The first automated classification of wall motion abnormalities (WMA) by using statistical knowledge of myocardial contours was presented by Bosch et. al. [78]. This CAD method utilized a statistical shape model (SSM) of endocardial contours, which was originally used for the segmentation of endocardial borders in echocardiograms [79]. A linear correlation was found between diagnostic predictors (active appearance motion model shape coefficients) with visual wall motion scores.

SSMs provide a morphometric analysis of biological shapes, which are characterized by a set of correspondent anatomical, geometrical or mathematical landmark points [80]. When a set of shapes from the same group is used to build the model, statistical inferences such as the mean shape and the modes of variation will only expose plausible shapes according to that group. The key problem is that the model needs to be specific enough to only generate representative examples. This is the underlying mechanism of Active Shape Models (ASM) [81], an automated segmentation method which has gained popularity for segmenting medical images in general [82, 83], and also for cardiac images [84–86].

SSMs require proper registration of training shapes to eliminate pose related variations (translation, scale and rotation). Post registration, SSMs will contain residual variations that only describe the true inter-subject differences. These variations should be small if all training shapes are taken from the same group, e.g., non pathological subjects. Fitting an SSM onto shapes from outside the model group may produce significantly large variations and errors. This particular feature becomes the main ingredient of characterizing normal and pathological shapes with SSMs [79, 87–89].

Parameterization of left ventricular (LV) motion appears to be a suitable approach to model myocardial contraction for CAD of ischaemia. Aside from SSMs, other CAD

approaches have been proposed to parameterize LV motion. A finite element model was introduced to parameterize wall motion [92]. A Hammer map projection was then applied to map the three-dimensional LV wall into continuous values of ischaemic zones: normal, hypokinesis, akinesis and dyskinesis. Finite element modeling was also combined with SSMs to estimate the deformation of the heart to distinguish normal and patients [91].

Other automated WMA classification methods include outlier detection in SSMs by inter-landmark distances [88], Hidden Markov Models [98], parametric imaging of wall motion[93, 95], linear classifiers [90, 96], and threshold-based LV function indicators [94]. A comparison of existing CAD methods for ischaemic heart disease based on wall motion analysis is given in Table 1.1.

1.3 Motivation and objectives

With the increasing prevalence and hospitalization rate of ischaemic heart disease, an explosive growth of diagnostic imaging for ischaemia is ongoing. Clinical decision making on revascularization procedures requires reliable viability assessment to assure long-term patient survival and to elevate cost effectiveness of the therapy and treatment. As such, the demand is increasing for a CAD method for ischaemic heart disease that supports clinicians with an objective analysis of infarct severity, a viability assessment or a prediction of potential functional improvement before performing revascularization.

The goal of this thesis was to explore novel mechanisms that can be used for CAD in ischemic heart disease, particularly through wall motion analysis from cardiac MR images. Existing diagnostic treatment of wall motion analysis from cardiac MR relies on visual wall motion scoring, which suffers from inter- and intra-observer variability. To minimize this variability, the automated method must contain essential knowledge on how the heart contracts normally. This enables quantification of hypokinetic myocardial segments, detection of segments with contractile reserve and prediction of functional improvement in stress. As such, the objectives of this thesis are threefold:

1. To find a proper shape parameterization for myocardial contraction. The dynamic nature of cardiac contraction must be represented in such a way that myocardial shapes from healthy subjects in this representation differ from shapes from ischaemic patients.

2. Define good descriptors and classifiers that are capable of detecting, locating and quantifying regional wall motion abnormalities (RWMA). Hence, locality is a key factor for providing automated segmental analysis of wall motion.

3. Investigate the possibility of applying the automated RWMA method for predicting regional functional improvement from rest to stress MR images.

1.4 Outline

This thesis is organized as follows.

Chapter 1 lays out the background and motivation of this thesis and presents a survey of current imaging techniques and CAD methods for ischaemic heart disease.

Chapter 2 describes a preliminary investigation on wall motion analysis to extract dense velocity vector fields from tagged MR imaging by using multiscale optic flow. This means velocity vectors from all pixels inside myocardium are automatically calculated over the full cardiac cycle. Quantitative validation is performed by comparing the estimated velocity vector fields with velocity-encoded (VEC) MRI.

Chapter 3 presents an exploratory study to find a proper shape representation for myocardial contraction. To model the dynamics of myocardial contraction in the static representation of SSMs, shape vectors are defined by serially concatenating endo- and epicardial contours at end-diastole (ED) with endo- and epicardial contours at end-systole (ES). Shapes from both healthy subjects and patients are combined into one SSM. Contractility patterns are extracted by using Principal Component Analysis (PCA) and Independent Component Analysis (ICA), and a comparison between the two decomposition methods is presented. In this chapter, the advantage of ICA to extract local shape features is demonstrated.

Chapter 4 gives the first application of ICA to detect regional wall motion abnormality (RWMA). Segments with abnormal wall motion are detected by the location of abnormal independent components (ICs) in myocardium. Qualitative evaluation of RWMA on six infarct patients is presented by correlating the position of abnormal ICs with hyperenhanced areas from the corresponding CE-MRI of the same patients.

Chapter 5: With the capability of ICA to detect RWMA for ischaemic patients as given in Chapter 4, we explored the method's potential use for predicting regional contractile improvement. Qualitative comparison of RWMA at rest with RWMA at stress is presented in this chapter. By comparing independent component coefficients from rest to stress, the potential to detect myocardial contractile improvement from rest to stress is investigated.

Chapter 6 represents the core of our CAD method for automated RWMA evaluation. The methodological formulation to estimate RWMA probability density functions is refined and improved by propagating the density functions from the independent component domain to the shape domain. This allows a direct quantification of RWMA at the landmark point level without the need to project a patient shape onto the ICA model. Quantitative validation results from 45 patients with ischaemic heart disease are also presented in this chapter.

Chapter 7: investigates of the possibility to automatically detect regional functional improvement when rest and stress cardiac MR data are combined. The statistical model is slightly adapted to accommodate the comparison between rest and stress data during the shapes alignment. A new evaluation of RWMA probability changes from rest to stress is proposed. Correlation with infarct transmuralities from CE-MRI is presented in this chapter.

Chapter 8 summarizes the CAD development for ischaemic heart disease. Future directions for building a computer-assisted cardiac ischaemia diagnosis method are presented at the end of this chapter.

1.5 References

[1] D. Lloyd-Jones, R. Adams, M. Carnethon, G. De Simone, T. B. Ferguson, K. Flegal, E. Ford, K. Furie, A. Go, K. Greenlund, N. Haase, S. Hailpern, M. Ho, V. Howard, B. Kissela, S. Kittner, D. Lackland, L. Lisabeth, A. Marelli, M. McDermott, J. Meigs, D. Mozaffarian, G. Nichol, C. O'Donnell, V. Roger, W. Rosamond, R. Sacco, P. Sorlie, R. Stafford, J. Steinberger, T. Thom, S. Wasserthiel-Smoller, N. Wong, J. Wylie-Rosett, and Y. Hong, "Heart disease and stroke statistics–2009 update: a report from the American Heart Association Statistics Committee and Stroke Statistics Subcommittee," *Circulation*, vol. 119, no. 3, pp. 480–486, Jan 2009.

[2] H. Mahrholdt, I. Klem, and U. Sechtem, "Cardiovascular MRI for detection of myocardial viability and ischaemia," *Heart*, vol. 93, no. 1, pp. 122–129, 2007.

[3] T. A. M. Kaandorp, H. J. Lamb, J. J. Bax, E. E. van der Wall, and A. de Roos, "Magnetic resonance imaging of coronary arteries, the ischemic cascade, and myocardial infarction." *Am Heart J*, vol. 149, no. 2, pp. 200–208, Feb 2005.

[4] G. P. Reddy, S. Pujadas, K. G. Ordovas, and C. B. Higgins, "MR imaging of ischemic heart disease," *Magn Reson Imaging Clin N Am*, vol. 16, no. 2, pp. 201–212, May 2008.

[5] G. Heusch, R. Schulz, and S. H. Rahimtoola, "Myocardial hibernation: a delicate balance," *Am J Physiol Heart Circ Physiol*, vol. 288, no. 3, pp. H984–99, Mar 2005.

[6] W. Wijns, S. F. Vatner, and P. G. Camici, "Hibernating myocardium," *N Engl J Med*, vol. 339, no. 3, pp. 173–181, Jul 1998.

[7] M. Jessup and S. Brozena, "Heart failure," *N Engl J Med*, vol. 348, no. 20, pp. 2007–2018, May 2003.

[8] S. H. Rahimtoola, V. Dilsizian, C. M. Kramer, T. H. Marwick, and J.-L. J. Vanoverschelde, "Chronic ischemic left ventricular dysfunction: from pathophysiology to imaging and its integration into clinical practice," *JACC Cardiovasc Imaging*, vol. 1, no. 4, pp. 536–555, Jul 2008.

[9] S. R. Underwood, J. J. Bax, J. vom Dahl, M. Y. Henein, J. Knuuti, A. C. van Rossum, E. R. Schwarz, J.-L. Vanoverschelde, E. E. van der Wall, and W. Wijns, "Imaging techniques for the assessment of myocardial hibernation. Report of a Study Group of the European Society of Cardiology," *Eur Heart J*, vol. 25, no. 10, pp. 815–836, May 2004.

[10] H. Sakuma, "Magnetic resonance imaging for ischemic heart disease," *J Magn Reson Imaging*, vol. 26, no. 1, pp. 3–13, Jul 2007.

[11] E. Wellnhofer, A. Olariu, C. Klein, M. Grafe, A. Wahl, E. Fleck, and E. Nagel, "Magnetic resonance low-dose dobutamine test is superior to SCAR quantification for the prediction of functional recovery," *Circulation*, vol. 109, no. 18, pp. 2172–2174, May 2004.

[12] T. D. Karamitsos, L. E. Hudsmith, J. B. Selvanayagam, S. Neubauer, and J. M. Francis, "Operator induced variability in left ventricular measurements with cardiovascular magnetic resonance is improved after training," *J Cardiovasc Magn Reson*, vol. 9, no. 5, pp. 777–783, 2007.

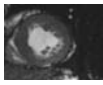

[13] I. Paetsch, C. Jahnke, V. A. Ferrari, F. E. Rademakers, P. A. Pellikka, W. G. Hundley, D. Poldermans, J. J. Bax, K. Wegscheider, E. Fleck, and E. Nagel, "Determination of interobserver variability for identifying inducible left ventricular wall motion abnormalities during dobutamine stress magnetic resonance imaging," *Eur Heart J*, vol. 27, no. 12, pp. 1459–1464, Jun 2006.

[14] F. M. Baer, E. Voth, C. A. Schneider, P. Theissen, H. Schicha, and U. Sechtem, "Comparison of low-dose dobutamine-gradient-echo magnetic resonance imaging and positron emission tomography with [18F]fluorodeoxyglucose in patients with chronic coronary artery disease. A functional and morphological approach to the detection of residual myocardial viability," *Circulation*, vol. 91, no. 4, pp. 1006–1015, 1995.

[15] F. M. Baer, P. Theissen, C. A. Schneider, E. Voth, U. Sechtem, H. Schicha, and E. Erdmann, "Dobutamine magnetic resonance imaging predicts contractile recovery of chronically dysfunctional myocardium after successful revascularization," *J Am Coll Cardiol*, vol. 31, no. 5, pp. 1040–1048, 1998.

[16] J. H. Cullen, M. A. Horsfield, C. R. Reek, G. R. Cherryman, D. B. Barnett, and N. J. Samani, "A myocardial perfusion reserve index in humans using first-pass contrast-enhanced magnetic resonance imaging," *J Am Coll Cardiol*, vol. 33, no. 5, pp. 1386–1394, Apr 1999.

[17] W. J. Manning, D. J. Atkinson, W. Grossman, S. Paulin, and R. R. Edelman, "First-pass nuclear magnetic resonance imaging studies using gadolinium-DTPA in patients with coronary artery disease," *J Am Coll Cardiol*, vol. 18, no. 4, pp. 959–965, Oct 1991.

[18] E. Nagel, C. Klein, I. Paetsch, S. Hettwer, B. Schnackenburg, K. Wegscheider, and E. Fleck, "Magnetic resonance perfusion measurements for the noninvasive detection of coronary artery disease," *Circulation*, vol. 108, no. 4, pp. 432–7, Jul 2003.

[19] A. Saraste, S. Nekolla, and M. Schwaiger, "Contrast-enhanced magnetic resonance imaging in the assessment of myocardial infarction and viability," *J Nucl Cardiol*, vol. 15, no. 1, pp. 105–117, Jan-Feb 2008.

[20] J. B. Selvanayagam, A. Kardos, J. M. Francis, F. Wiesmann, S. E. Petersen, D. P. Taggart, and S. Neubauer, "Value of Delayed-Enhancement Cardiovascular Magnetic Resonance Imaging in Predicting Myocardial Viability After Surgical Revascularization," *Circulation*, vol. 110, no. 12, pp. 1535–1541, Sep 2004.

[21] L. Van Hoe and M. Vanderheyden, "Ischemic cardiomyopathy: value of different MRI techniques for prediction of functional recovery after revascularization," *AJR Am J Roentgenol*, vol. 182, no. 1, pp. 95–100, Jan 2004.

[22] P. R. Schvartzman, M. B. Srichai, R. A. Grimm, N. A. Obuchowski, D. F. Hammer, P. M. McCarthy, J. M. Kasper, and R. D. White, "Nonstress delayed-enhancement magnetic resonance imaging of the myocardium predicts improvement of function after revascularization for chronic ischemic heart disease with left ventricular dysfunction," *Am Heart J*, vol. 146, no. 3, pp. 535–541, Sep 2003.

[23] H. P. Kuhl, C. S. A. Lipke, G. A. Krombach, M. Katoh, T. F. Battenberg, B. Nowak, N. Heussen, A. Buecker, and W. M. Schaefer, "Assessment of reversible myocardial dysfunction in chronic ischaemic heart disease: comparison of contrast-enhanced cardiovascular magnetic resonance and a combined positron emission tomography-single photon emission computed tomography imaging protocol," *Eur Heart J*, vol. 27, no. 7, pp. 846–853, Apr 2006.

[24] M. Gutberlet, M. Frohlich, S. Mehl, H. Amthauer, H. Hausmann, R. Meyer, H. Siniawski, J. Ruf, M. Plotkin, T. Denecke, B. Schnackenburg, R. Hetzer, and R. Felix, "Myocardial viability assessment in patients with highly impaired left ventricular function: Comparison of delayed enhancement, dobutamine stress MRI, end-diastolic wall thickness, and TI201-SPECT with functional recovery after revascularization," *Eur Radiol*, vol. 15, no. 5, pp. 872–880, May 2005.

[25] D. S. McLean, A. V. Anadiotis, and S. Lerakis, "Role of echocardiography in the assessment of myocardial viability," *Am J Med Sci*, vol. 337, no. 5, pp. 349–354, May 2009.

[26] S. A. Mollema, G. Nucifora, and J. J. Bax, "Prognostic value of echocardiography after acute myocardial infarction," *Heart*, Mar 2009.

[27] J. Meluzin, C. G. Cigarroa, M. E. Brickner, J. Cerny, L. Spinarova, M. Frelich, F. Stetka, L. Groch, and P. A. Grayburn, "Dobutamine echocardiography in predicting improvement in global left ventricular systolic function after coronary bypass or angioplasty in patients with healed myocardial infarcts," *Am J Cardiol*, vol. 76, no. 12, pp. 877–880, Nov 1995.

[28] R. Hoffmann, H. Lethen, T. Marwick, M. Arnese, P. Fioretti, A. Pingitore, E. Picano, T. Buck, R. Erbel, F. A. Flachskampf, and P. Hanrath, "Analysis of interinstitutional observer agreement in interpretation of dobutamine stress echocardiograms," *J Am Coll Cardiol*, vol. 27, no. 2, pp. 330–336, Feb 1996.

[29] E. Picano, F. Lattanzi, A. Orlandini, C. Marini, and A. L'Abbate, "Stress echocardiography and the human factor: the importance of being expert," *J Am Coll Cardiol*, vol. 17, no. 3, pp. 666–669, Mar 1991.

[30] R. Hoffmann, H. Lethen, T. Marwick, R. Rambaldi, P. Fioretti, A. Pingitore, E. Picano, T. Buck, R. Erbel, F. A. Flachskampf, and P. Hanrath, "Standardized guidelines for the interpretation of dobutamine echocardiography reduce interinstitutional variance in interpretation," *Am J Cardiol*, vol. 82, no. 12, pp. 1520–1524, Dec 1998.

[31] A. Nemes, K. Y. E. Leung, G. van Burken, M. van Stralen, J. G. Bosch, O. I. I. Soliman, B. J. Krenning, W. B. Vletter, F. J. ten Cate, and M. L. Geleijnse, "Side-by-side viewing of anatomically aligned left ventricular segments in three-dimensional stress echocardiography." *Echocardiography*, vol. 26, no. 2, pp. 189–195, Feb 2009.

[32] G. R. Sutherland, M. J. Stewart, K. W. Groundstroem, C. M. Moran, A. Fleming, F. J. Guell-Peris, R. A. Riemersma, L. N. Fenn, K. A. Fox, and W. N. McDicken, "Color Doppler myocardial imaging: a new technique for the assessment of myocardial function," *J Am Soc Echocardiogr*, vol. 7, no. 5, pp. 441–458, Sep-Oct 1994.

[33] J. Chan, L. Hanekom, C. Wong, R. Leano, G.-Y. Cho, and T. H. Marwick, "Differentiation of subendocardial and transmural infarction using two-dimensional strain rate imaging to assess short-axis and long-axis myocardial function," *J Am Coll Cardiol*, vol. 48, no. 10, pp. 2026–2033, Nov 2006.

[34] K. Wita, A. Filipecki, A. Drzewiecka-Gerber, M. Turski, A. Rybicka-Musialik, Z. Tabor, M. Nowak, W. Wrobel, J. Krauze, J. Szczogiel, and M. Trusz-Gluza, "The use of myocardial contrast echocardiography in the assessment of left ventricular function recovery after primary percutaneous coronary intervention in the setting of acute myocardial infarction," *Kardiol Pol*, vol. 64, no. 7, pp. 713–721, Jul 2006.

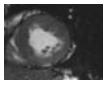

[35] J. J. Bax, F. C. Visser, A. van Lingen, J. H. Cornel, P. M. Fioretti, and E. E. van der Wall, "Metabolic imaging using F18-fluorodeoxyglucose to assess myocardial viability," *Int J Card Imaging*, vol. 13, no. 2, pp. 145–155, Apr 1997.

[36] V. Dilsizian and R. O. Bonow, "Current diagnostic techniques of assessing myocardial viability in patients with hibernating and stunned myocardium," *Circulation*, vol. 87, no. 1, pp. 1–20, Jan 1993.

[37] D. W. Townsend, "Dual-modality imaging: combining anatomy and function," *J Nucl Med*, vol. 49, no. 6, pp. 938–955, Jun 2008.

[38] E. Inglese, L. Leva, R. Matheoud, G. Sacchetti, C. Secco, P. Gandolfo, M. Brambilla, and G. Sambuceti, "Spatial and temporal heterogeneity of regional myocardial uptake in patients without heart disease under fasting conditions on repeated whole-body 18F-FDG PET/CT," *J Nucl Med*, vol. 48, no. 10, pp. 1662–1669, Oct 2007.

[39] G. Brix, E. A. Nekolla, D. Nosske, and J. Griebel, "Risks and safety aspects related to PET/MR examinations," *Eur J Nucl Med Mol Imaging*, vol. 36 Suppl 1, pp. S131–8, Mar 2009.

[40] P. Kaufmann, "Cardiac hybrid imaging: state-of-the-art." *Ann Nucl Med*, Apr 2009.

[41] S. G. Nekolla, A. Martinez-Moeller, and A. Saraste, "PET and MRI in cardiac imaging: from validation studies to integrated applications," *Eur J Nucl Med Mol Imaging*, vol. 36 Suppl 1, pp. S121–30, Mar 2009.

[42] A. K. Paul and H. A. Nabi, "Gated myocardial perfusion SPECT: basic principles, technical aspects, and clinical applications," *J Nucl Med Technol*, vol. 32, no. 4, pp. 179–187, Dec 2004.

[43] V. Go, M. R. Bhatt, and R. C. Hendel, "The diagnostic and prognostic value of ECG-gated SPECT myocardial perfusion imaging," *J Nucl Med*, vol. 45, no. 5, pp. 912–921, May 2004.

[44] A. Maruyama, S. Hasegawa, A. K. Paul, M. Xiuli, J. Yoshioka, K. Maruyama, M. Hori, and T. Nishimura, "Myocardial viability assessment with gated SPECT Tc-99m tetrofosmin % wall thickening: comparison with F-18 FDG-PET," *Ann Nucl Med*, vol. 16, no. 1, pp. 25–32, Feb 2002.

[45] M. G. Levine, C. C. McGill, A. W. Ahlberg, M. P. White, S. Giri, B. Shareef, D. Waters, and G. V. Heller, "Functional assessment with electrocardiographic gated single-photon emission computed tomography improves the ability of technetium-99m sestamibi myocardial perfusion imaging to predict myocardial viability in patients undergoing revascularization," *Am J Cardiol*, vol. 83, no. 1, pp. 1–5, Jan 1999.

[46] W. J. Kang, D. S. Lee, J. C. Paeng, K.-B. Kim, J.-K. Chung, and M. C. Lee, "Prognostic value of rest (201)Tl-dipyridamole stress (99m)Tc-sestamibi gated SPECT for predicting patient-based clinical outcomes after bypass surgery in patients with ischemic left ventricular dysfunction," *J Nucl Med*, vol. 44, no. 11, pp. 1735–1740, Nov 2003.

[47] J. Taki, T. Higuchi, K. Nakajima, I. Matsunari, E.-H. Hwang, H. Bunko, M. Kawasuji, G. Watanabe, and N. Tonami, "Electrocardiographic gated (99m)Tc-MIBI SPECT for functional assessment of patients after coronary artery bypass surgery: comparison of wall thickening and wall motion analysis," *J Nucl Med*, vol. 43, no. 5, pp. 589–595, May 2002.

[48] S. Hida, T. Chikamori, Y. Usui, H. Yanagisawa, T. Morishima, and A. Yamashina, "Effect of percutaneous coronary angioplasty on myocardial perfusion, function, and wall thickness as assessed by quantitative gated single-photon emission computed tomography," *Am J Cardiol*, vol. 91, no. 5, pp. 591–594, Mar 2003.

[49] P. H. Meyers, C. M. Nice, Jr, H. C. Becker, W. J. Nettleton, Jr, J. W. Sweeney, and G. R. Meckstroth, "Automated computer analysis of radiographic images," *Radiology*, vol. 83, pp. 1029–34, Dec 1964.

[50] G. S. Lodwick, A. H. Turner, Jr, L. B. Lusted, and A. W. Templeton, "Computer-aided analysis of radiographic images," *J Chronic Dis*, vol. 19, no. 4, pp. 485–96, Apr 1966.

[51] R. L. Engle, Jr, "Attempts to use computers as diagnostic aids in medical decision making: a thirty-year experience," *Perspect Biol Med*, vol. 35, no. 2, pp. 207–19, 1992.

[52] B. van Ginneken, B. M. ter Haar Romeny, and M. A. Viergever, "Computer-aided diagnosis in chest radiography: a survey." *IEEE Trans Med Imaging*, vol. 20, no. 12, pp. 1228–1241, Dec 2001.

[53] C. S. White, R. Pugatch, T. Koonce, S. W. Rust, and E. Dharaiya, "Lung nodule CAD software as a second reader: a multicenter study," *Acad Radiol*, vol. 15, no. 3, pp. 326–333, Mar 2008.

[54] J. J. Chen and C. S. White, "Use of CAD to evaluate lung cancer on chest radiography," *J Thorac Imaging*, vol. 23, no. 2, pp. 93–96, May 2008.

[55] T. Mang, P. Peloschek, C. Plank, A. Maier, A. Graser, M. Weber, C. Herold, L. Bogoni, and W. Schima, "Effect of computer-aided detection as a second reader in multidetector-row CT colonography," *Eur Radiol*, vol. 17, no. 10, pp. 2598–607, Oct 2007.

[56] B. Sahiner, H.-P. Chan, L. M. Hadjiiski, P. N. Cascade, E. A. Kazerooni, A. R. Chughtai, C. Poopat, T. Song, L. Frank, J. Stojanovska, and A. Attili, "Effect of CAD on radiologists' detection of lung nodules on thoracic CT scans: analysis of an observer performance study by nodule size," *Acad Radiol*, vol. 16, no. 12, pp. 1518–30, Dec 2009.

[57] S. Halligan, D. G. Altman, S. Mallett, S. A. Taylor, D. Burling, M. Roddie, L. Honeyfield, J. McQuillan, H. Amin, and J. Dehmeshki, "Computed tomographic colonography: assessment of radiologist performance with and without computer-aided detection," *Gastroenterology*, vol. 131, no. 6, pp. 1690–9, Dec 2006.

[58] N. Petrick, M. Haider, R. M. Summers, S. C. Yeshwant, L. Brown, E. M. Iuliano, A. Louie, J. R. Choi, and P. J. Pickhardt, "CT colonography with computer-aided detection as a second reader: observer performance study," *Radiology*, vol. 246, no. 1, pp. 148–156, Jan 2008.

[59] M. E. Baker, L. Bogoni, N. A. Obuchowski, C. Dass, R. M. Kendzierski, E. M. Remer, D. M. Einstein, P. Cathier, A. Jerebko, S. Lakare, A. Blum, D. F. Caroline, and M. Macari, "Computer-aided detection of colorectal polyps: can it improve sensitivity of less-experienced readers? preliminary findings," *Radiology*, vol. 245, no. 1, pp. 140–9, Oct 2007.

[60] L. Bogoni, P. Cathier, M. Dundar, A. Jerebko, S. Lakare, J. Liang, S. Periaswamy, M. E. Baker, and M. Macari, "Computer-aided detection (CAD) for CT colonography: a tool to address a growing need," *Br J Radiol*, vol. 78 Spec No 1, pp. S57–62, 2005.

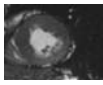

[61] D. Georgian-Smith, R. H. Moore, E. Halpern, E. D. Yeh, E. A. Rafferty, H. A. D'Alessandro, M. Staffa, D. A. Hall, K. A. McCarthy, and D. B. Kopans, "Blinded comparison of computer-aided detection with human second reading in screening mammography," *AJR Am J Roentgenol*, vol. 189, no. 5, pp. 1135–1141, Nov 2007.

[62] N. Karssemeijer, A. M. Bluekens, D. Beijerinck, J. J. Deurenberg, M. Beekman, R. Visser, R. van Engen, A. Bartels-Kortland, and M. J. Broeders, "Breast cancer screening results 5 years after introduction of digital mammography in a population-based screening program," *Radiology*, vol. 253, no. 2, pp. 353–8, Nov 2009.

[63] J. Tang, R. M. Rangayyan, J. Xu, I. El Naqa, and Y. Yang, "Computer-aided detection and diagnosis of breast cancer with mammography: recent advances," *IEEE Trans Inf Technol Biomed*, vol. 13, no. 2, pp. 236–51, Mar 2009.

[64] K. Doi, "Computer-aided diagnosis in medical imaging: historical review, current status and future potential," *Comput Med Imaging Graph*, vol. 31, no. 4-5, pp. 198–211, 2007.

[65] M. L. Giger, H.-P. Chan, and J. Boone, "Anniversary paper: History and status of CAD and quantitative image analysis: the role of Medical Physics and AAPM," *Med Phys*, vol. 35, no. 12, pp. 5799–820, Dec 2008.

[66] D. Hock, R. Ouhadi, R. Materne, A.-S. Aouchria, I. Mancini, T. Broussaud, P. Magotteaux, and A. Nchimi, "Virtual dissection CT colonography: evaluation of learning curves and reading times with and without computer-aided detection," *Radiology*, vol. 248, no. 3, pp. 860–8, Sep 2008.

[67] F. Beyer, L. Zierott, E. M. Fallenberg, K. U. Juergens, J. Stoeckel, W. Heindel, and D. Wormanns, "Comparison of sensitivity and reading time for the use of computer-aided detection (cad) of pulmonary nodules at mdct as concurrent or second reader," *Eur Radiol*, vol. 17, no. 11, pp. 2941–7, Nov 2007.

[68] D. Bielen and G. Kiss, "Computer-aided detection for ct colonography: update 2007," *Abdom Imaging*, vol. 32, no. 5, pp. 571–81, 2007.

[69] M. Freedman and T. Osicka, "Reader variability: what we can learn from computer-aided detection experiments," *J Am Coll Radiol*, vol. 3, no. 6, pp. 446–55, Jun 2006.

[70] T. Hirai, Y. Korogi, H. Arimura, S. Katsuragawa, M. Kitajima, M. Yamura, Y. Yamashita, and K. Doi, "Intracranial aneurysms at MR angiography: effect of computer-aided diagnosis on radiologists' detection performance," *Radiology*, vol. 237, no. 2, pp. 605–10, Nov 2005.

[71] S. Kakeda, Y. Korogi, H. Arimura, T. Hirai, S. Katsuragawa, T. Aoki, and K. Doi, "Diagnostic accuracy and reading time to detect intracranial aneurysms on MR angiography using a computer-aided diagnosis system," *AJR Am J Roentgenol*, vol. 190, no. 2, pp. 459–65, Feb 2008.

[72] S. Buhmann, P. Herzog, J. Liang, M. Wolf, M. Salganicoff, C. Kirchhoff, M. Reiser, and C. H. Becker, "Clinical evaluation of a computer-aided diagnosis (CAD) prototype for the detection of pulmonary embolism," *Acad Radiol*, vol. 14, no. 6, pp. 651–8, Jun 2007.

[73] Y. Hatanaka, T. Nakagawa, A. Aoyama, X. Zhou, T. Hara, H. Fujita, M. Kakogawa, Y. Hayashi, Y. Mizukusa, and A. Fujita, "Automated detection algorithm for arteriolar narrowing on fundus images," *Conf Proc IEEE Eng Med Biol Soc*, vol. 1, pp. 286–9, 2005.

[74] R. J. van der Geest and J. H. Reiber, "Quantification in cardiac MRI," *J Magn Reson Imaging*, vol. 10, no. 5, pp. 602–608, Nov 1999.

[75] P. Balzer, A. Furber, S. Delepine, F. Rouleau, F. Lethimonnier, O. Morel, A. Tadei, P. Jallet, P. Geslin, and J. J. le Jeune, "Regional assessment of wall curvature and wall stress in left ventricle with magnetic resonance imaging," *Am J Physiol*, vol. 277, no. 3 Pt 2, pp. H901–10, Sep 1999.

[76] A. F. Frangi, W. J. Niessen, and M. A. Viergever, "Three-dimensional modeling for functional analysis of cardiac images: a review," *IEEE Trans Med Imaging*, vol. 20, no. 1, pp. 2–25, Jan 2001.

[77] A. A. Young and A. F. Frangi, "Computational cardiac atlases: from patient to population and back," *Exp Physiol*, vol. 94, no. 5, pp. 578–596, May 2009.

[78] J. G. Bosch, F. Nijland, S. C. Mitchell, B. P. F. Lelieveldt, O. Kamp, J. H. C. Reiber, and M. Sonka, "Computer-aided diagnosis via model-based shape analysis: automated classification of wall motion abnormalities in echocardiograms," *Acad Radiol*, vol. 12, no. 3, pp. 358–367, Mar 2005.

[79] J. G. Bosch, S. C. Mitchell, B. P. F. Lelieveldt, F. Nijland, O. Kamp, M. Sonka, and J. H. C. Reiber, "Automatic segmentation of echocardiographic sequences by active appearance motion models," *IEEE Trans Med Imaging*, vol. 21, no. 11, pp. 1374–1383, Nov 2002.

[80] I. L. Dryden and K. V. Mardia, *Statistical Shape Analysis*. John Wiley & Sons, Inc., 1998.

[81] T. Cootes, D. Cooper, C. Taylor, and J. Graham, "Active Shape Models - their training and application," *Computer Vision and Image Understanding*, vol. 61, no. 1, pp. 38–59, Jan 1995.

[82] C. J. Taylor, T. F. Cootes, A. Lanitis, G. Edwards, P. Smyth, and A. C. Kotcheff, "Model-based interpretation of complex and variable images," *Philos Trans R Soc Lond B Biol Sci*, vol. 352, no. 1358, pp. 1267–1274, Aug 1997.

[83] T. F. Cootes and C. J. Taylor, "Anatomical statistical models and their role in feature extraction," *Br J Radiol*, vol. 77 Spec No 2, pp. S133–9, 2004.

[84] S. C. Mitchell, J. G. Bosch, B. P. F. Lelieveldt, R. J. van der Geest, J. H. C. Reiber, and M. Sonka, "3-D active appearance models: segmentation of cardiac MR and ultrasound images," *IEEE Trans Med Imaging*, vol. 21, no. 9, pp. 1167–1178, Sep 2002.

[85] H. van Assen, M. Danilouchkine, A. Frangi, S. Ordas, J. Westenberg, J. Reiber, and B. Lelieveldt, "SPASM: A 3D-ASM for segmentation of sparse and arbitrarily oriented cardiac MRI data," *Medical Image Analysis*, vol. 10, no. 2, pp. 286–303, APR 2006.

[86] A. Andreopoulos and J. K. Tsotsos, "Efficient and generalizable statistical models of shape and appearance for analysis of cardiac MRI," *Med Image Anal*, vol. 12, no. 3, pp. 335–357, Jun 2008.

[87] S. C. Mitchell, B. P. F. Lelieveldt, H. G. Bosch, J. H. C. Reiber, and M. Sonka, "Disease characterization of active appearance model coefficients," in *Proc. SPIE Medical Imaging 2003, Vol. 5032*, M. Sonka and J. M. Fitzpatrick, Eds., San Diego, USA, May 2003, pp. 38–49.

[88] K. Lekadir, R. Merrifield, and G.-Z. Yang, "Outlier detection and handling for robust 3-D active shape models search," *IEEE Trans Med Imaging*, vol. 26, no. 2, pp. 212–222, Feb 2007.

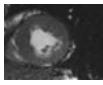

[89] M. Sonka, J. G. Bosch, B. P. Lelieveldt, S. C. Mitchell, and J. H. Reiber, "Computer-aided diagnosis via model-based shape analysis: cardiac MR and Echo," in *Computer Assisted Radiology and Surgery (CARS) 2003*, ser. International Congress Series, vol. 1256, Jun 2003, pp. 1013–1018.

[90] K. H. Douglass, J. M. Links, D. C. Chen, D. F. Wong, and H. N. J. Wagner, "Linear discriminant analysis of regional ejection fractions in the diagnosis of coronary artery disease." *Eur J Nucl Med*, vol. 12, no. 12, pp. 602–604, 1987.

[91] E. W. Remme, A. A. Young, K. F. Augenstein, B. Cowan, and P. J. Hunter, "Extraction and quantification of left ventricular deformation modes," *IEEE Trans Biomed Eng*, vol. 51, no. 11, pp. 1923–1931, Nov 2004.

[92] S. L. Herz, C. M. Ingrassia, S. Homma, K. D. Costa, and J. W. Holmes, "Parameterization of left ventricular wall motion for detection of regional ischemia," *Annals of Biomedical Engineering*, vol. 33, no. 7, pp. 912–919, Jul 2005.

[93] C. Ruiz Dominguez, N. Kachenoura, A. De Cesare, A. Delouche, P. Lim, O. Gerard, A. Herment, B. Diebold, and F. Frouin, "Assessment of left ventricular contraction by parametric analysis of main motion (PAMM): theory and application for echocardiography," *Phys Med Biol*, vol. 50, no. 14, pp. 3277–3296, Jul 2005.

[94] E. G. Caiani, E. Toledo, P. MacEneaney, D. Bardo, S. Cerutti, R. M. Lang, and V. Mor-Avi, "Automated interpretation of regional left ventricular wall motion from cardiac magnetic resonance images," *J Cardiovasc Magn Reson*, vol. 8, no. 3, pp. 427–433, 2006.

[95] N. Kachenoura, A. Redheuil, D. Balvay, C. Ruiz-Dominguez, A. Herment, E. Mousseaux, and F. Frouin, "Evaluation of regional myocardial function using automated wall motion analysis of cine MR images: Contribution of parametric images, contraction times, and radial velocities," *J Magn Reson Imaging*, vol. 26, no. 4, pp. 1127–1132, Oct 2007.

[96] M. Qazi, G. Fung, S. Krishnan, J. Bi, R. B. Rao, and A. S. Katz, "Automated heart abnormality detection using sparse linear classifiers," *IEEE Eng Med Biol Mag*, vol. 26, no. 2, pp. 56–63, Mar-Apr 2007.

[97] K. Y. E. Leung and J. G. Bosch, "Segmental wall motion classification in echocardiograms using compact shape descriptors," *Acad Radiol*, vol. 15, no. 11, pp. 1416–1424, Nov 2008.

[98] S. Mansor, N. P. Hughes, and J. A. Noble, "Wall motion classification of stress echocardiography based on combined rest-and-stress data," *Med Image Comput Comput Assist Interv Int Conf Med Image Comput Comput Assist Interv*, vol. 11, no. Pt 2, pp. 139–146, 2008.

[99] A. Suinesiaputra, A. F. Frangi, H. J. Lamb, J. H. C. Reiber, and B. P. F. Lelieveldt, "Automatic prediction of myocardial contractility improvement in stress MRI using shape morphometrics with independent component analysis," *Inf Process Med Imaging*, vol. 19, pp. 321–332, 2005.

[100] A. Suinesiaputra, A. F. Frangi, T. A. M. Kaandorp, H. J. Lamb, J. J. Bax, J. H. C. Reiber, and B. P. F. Lelieveldt, "Automated detection of regional wall motion abnormalities based on a statistical model applied to multislice short-axis cardiac MR images," *IEEE Trans Med Imaging*, vol. 28, no. 4, pp. 595–607, Apr 2009.